Electrostatic Modification of the Active Site of Myoglobin: Characterization of the Proximal Ser92Asp Variant†

Emma Lloyd,‡,§ David L. Burk,‡ Juan C. Ferrer,‡,|| Robert Maurus,‡ John Doran,⊥ Paul R. Carey,#,▽ Gary D. Brayer,‡ and A. Grant Mauk*,‡

Department of Biochemistry and Molecular Biology and the Protein Engineering Network of Centres of Excellence, University of British Columbia, Vancouver, British Columbia, Canada V6T 1Z3, Department of Biochemistry, University of Ottawa, Ottawa, Ontario, Canada K1N 6N5, and Institute for Biological Sciences, National Research Council, Ottawa, Ontario, Canada K1A OR6

Received April 15, 1996; Revised Manuscript Received June 17, 1996⊗

ABSTRACT: The structural and functional consequences of the introduction of a negatively charged amino acid into the active site of horse heart myoglobin have been investigated by replacement of the proximal Ser92 residue (F7) with an aspartyl residue (Ser92Asp). UV−visible absorption maxima of various ferrous and ferric derivatives and low-temperature EPR spectra of the metaquo (metMb) derivative indicate that the active site coordination geometry has not been perturbed significantly in the variant. ^{1}H-NMR spectroscopy provides direct evidence for the existence of a distal water molecule as the sixth ligand in the oxidized form of the variant at pD 5.7. Spectrophotometric pH titration of the Ser92Asp variant is consistent with this finding and with a pK_a = 8.90 ± 0.02 [25.0 °C, μ = 0.10 M (NaCl)] for titration of the distal water molecule, identical to the value reported for the wild-type protein. X-ray crystallography of the metMb derivative indicates that the heme substituents conserve their orientations in the variant protein, except for a slight reorientation of the pyrrole A propionate group to which Ser92 normally hydrogen bonds and reorientation of the carboxyl end of the pyrrole D propionate group. No change is observed in conformation of the proximal (His93) or distal (Wat156) heme ligands. ^{1}H-NMR spectroscopy of the metMbCN form of the protein indicates that a slight rotation of the proximal His93 ligand has occurred in this derivative. Resonance Raman experiments indicate increased conformational heterogeneity in the proximal pocket of the variant. Failure to detect electron density for the Asp residue in the X-ray diffraction map of the variant protein and high average thermal factors for the pyrrole A propionate substituent are consistent with this observation. The variant exhibits novel pH-dependent behavior in the metMb form, as shown by ^{1}H-NMR spectroscopy, and provides evidence for a heme-linked titratable group with a pK_a of 5.4 in this derivative. The metMbCN and deoxyMb derivatives also exhibit pH-dependent behavior, with pK_as of 5.60 ± 0.07 and 6.60 ± 0.07, respectively, compared to the wild-type values of 5.4 ± 0.04 and 5.8 ± 0.1. The heme-linked ionizable group is proposed to be His97 in all three derivatives. The reduction potential of the variant is 72 ± 2 mV *vs* SHE [25.0 °C, μ = 0.10 M (phosphate), pH 6.0], an increase of 8 mV over the wild-type value. The possible influence of a number of variables on the magnitude of the reduction potential in myoglobin and other heme proteins is discussed.

Myoglobin is a small heme-containing protein (M_r ∼ 17 800) that functions as a reversible oxygen carrier (Wittenberg, 1970; Wittenberg et al., 1975) and has long been the subject of intense investigation (Antonini & Brunori, 1971; Ho, 1982). With the advent of site-directed mutagenesis, the roles of individual amino acids can be addressed, and in this sense, much recent interest has focused on ligand binding properties of myoglobin variants, and in particular on the influence of the distal His64 (E7) ligand (Bellelli et al., 1990; Rohlfs et al., 1990; Sato et al., 1990; Carver et al., 1990; Saito et al., 1991, 1992, 1993; Sakan et al., 1993) and the distal Val68 (E11) (Egeberg et al., 1990; Smerdon et al., 1991; Cameron et al., 1993) residues.

One aspect of myoglobin that remains relatively unexplored is the effect of the introduction of potentially charged amino acids into the hydrophobic heme pocket. It is widely accepted that charged amino acids have important implications for the active site chemistry and functional properties of heme proteins in general. An intriguing extension to this general concept relates to the ability of charged groups to alter the oxidation−reduction properties of the heme iron (Moore & Williams, 1977; Moore et al., 1986); however, the operative mechanisms remain as yet only poorly defined, and the emphasis of relevant studies has been restricted for the most part to electron-transfer metalloproteins rather than the oxygen carriers. Hence, although the influence of surface charge substitution has been addressed in cytochrome b_5

† This work was supported by the Protein Engineering Network of Centres of Excellence. The NMR spectrometer was supported by MRC of Canada Maintenance Grant ME-7826 (to Professor P. R. Cullis). R.M. is a recipient of an MRC of Canada Studentship.

‡ University of British Columbia.

§ Present address: Department of Chemistry, University of Leicester, Leicester, LE1 7RH U.K.

|| Present address: Unitat de Bioquímica y Biologia Molecular, Departament de Bioquímica y Biologia Molecular, Facultat de Química, Universitat de Barcelona, Martí I Franquès, 1, 08028 Barcelona, Spain.

⊥ University of Ottawa.

National Research Council.

▽ Present address: Department of Biochemistry, Case Western Reserve University, 10900 Euclid Avenue, Cleveland, Ohio 44106-4935.

⊗ Abstract published in *Advance ACS Abstracts,* August 15, 1996.

S0006-2960(96)00897-5 CCC: $12.00

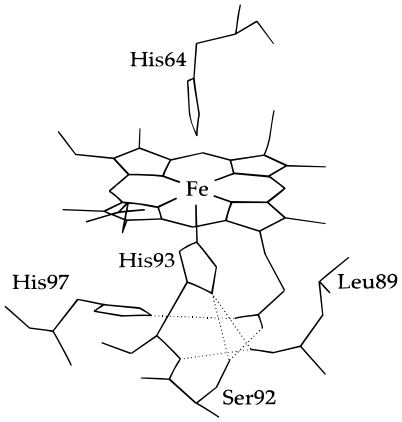

FIGURE 1: Active site of horse heart myoglobin. Hydrogen bonds (dotted lines) involving the NE1 of His97, the heme 7-propionate, the ND1 H of His93, the carbonyl group of Leu89, and the OG of Ser92 are indicated.

(Rodgers & Sligar, 1991; Northrup et al., 1993), and the effect of charge substitution close to an internal hydrophilic region containing the heme propionates of cytochrome *c* has also been examined (Moore et al., 1984; Cutler et al., 1989; Davies et al., 1993), the specific issue of *active site* charge substitutions in myoglobin has emphasized substitutions in the distal heme pocket (Varadarajan et al., 1989a,b; Zewert et al., 1994).

In horse heart myoglobin, Ser92 (F7) is located directly adjacent to the proximal His93 ligand (Figure 1) and is part of an extensive hydrogen-bonding network that involves Ser92, His93, His97, the heme pyrrole A propionate, and Leu89 (Evans & Brayer, 1990). As part of a multidisciplinary series of structural, spectroscopic, and mechanistic investigations into the effects of charged amino acid substitutions at the active site of myoglobin, a variant has been constructed in which the proximal Ser92 residue has been replaced with an aspartyl residue (Ser92Asp). In the present study, a variety of techniques has been used to characterize the structural, spectroscopic, and functional consequences of this substitution. As discussed below, the effects of this proximal substitution differ significantly from those resulting from the related modification of the distal heme binding pocket (Varadarajan et al., 1989a,b; Zewert et al., 1994).

EXPERIMENTAL PROCEDURES

Mutagenesis and Protein Expression. Oligonucleotide-directed mutagenesis (Zoller & Smith, 1987) and the expression of a synthetic gene for horse heart myoglobin (Guillemette et al., 1991) have been described. The oligonucleotide sequence used in preparing the Ser92Asp variant was 5′-GTGTTTAGTAGCATGGTCTTGCGCAAGCGG-3′ with the 5′ end phosphorylated and with the bases underlined indicating the mutation site. After mutagenesis, the entire gene was sequenced (Guillemette et al., 1991) to confirm the fidelity of the Ser92Asp mutation.

Protein Purification. Purification of the Ser92Asp variant devoid of contaminating sulfmyoglobin was performed as reported for the wild-type protein (Guillemette et al., 1991; Lloyd & Mauk, 1994). Purified protein had an *R* value ($A_{408.5}/A_{280}$) of ≥5.3 (pH 6.0, 25.0 °C) and migrated as a single band on SDS−PAGE. Absorption coefficients were determined using the pyridine−hemochromogen method (Antonini & Brunori, 1971; de Duve, 1948; Paul et al., 1953). DeoxyMb was prepared by addition of a small excess of solid sodium dithionite, and CO-bound samples were prepared by bubbling of deoxyMb gently with CO. The anion-bound adducts of the variant (metMbN_3^-, metMbCN^-, and metMbF^-) were obtained by addition of excess NaN_3, KCN, or KF to metMb.

Mass Spectrometry. Electrospray mass spectrometry (Feng et al., 1992) was performed as described previously (Lloyd & Mauk, 1994).

Determination of Distal Water pK_a. The electronic spectrum of a sample of metMb in 0.10 M NaCl (pH ∼6.0, 25.0 °C) was monitored as the pH of the solution was adjusted by incremental addition (≤2 μL) of 0.10 M NaOH. Electronic spectra were recorded with a Cary 219 spectrophotometer interfaced to a microcomputer (OLIS, Bogart, GA) and fitted with a circulating thermostatted water bath. The pH of the sample was recorded before and after measurement of the spectrum. The nonlinear least squares fitting program Minsq v.4.02 (MicroMath) was used to fit the data to the Henderson−Hasselbach equation (eq 1) for a one-proton process:

$$Z = [A + B \times 10^{(\mathrm{pH}-\mathrm{p}K)}]/[1 + 10^{(\mathrm{pH}-\mathrm{p}K)}] \qquad (1)$$

where *Z* is the absorbance and *A* and *B* are the absorbancies of the acidic and basic forms, respectively.

EPR Spectroscopy. EPR spectra were obtained with a Bruker ESP 300E spectrometer equipped with an Oxford Instruments Model 900 liquid helium cryostat, an Oxford Instruments Model ITC4 temperature controller, a Bruker Model ER035M gauss meter, and a Hewlett-Packard Model 5352B frequency counter. Samples of metMb (∼1 mM) were prepared by exchanging the protein into 0.10 M NaCl and adjusting the pH to 10.0 by addition of 0.10 M NaOH.

Spectroelectrochemistry. Reduction potentials (25.0 °C, pH 6.0, μ = 0.10 M) were obtained using an optically transparent thin-layer electrode (OTTLE) (Heineman et al., 1975; Reid et al., 1982) with recrystallized $[Ru(NH_3)_6]Cl_3$ (Alfa; Pladzewicz et al., 1973), as mediator. Spectra were collected with a Cary 219 spectrophotometer as described above. Potentiometric data were fitted (Minsq v.4.02; MicroMath, Orem, UT) to the Nernst equation following conversion of measured potentials to the hydrogen scale (Dutton, 1978).

^{1}H-NMR Spectroscopy. ^{1}H-NMR spectra were recorded at 20 °C with a Bruker MSL-200 spectrometer operating in the quadrature mode at 200 MHz. For the high-spin derivatives (metMb and deoxyMb), spectra were obtained by collecting 20 000 transients over a 62.5 kHz band width with 8192 data points using a superWEFT sequence (Inubushi & Becker, 1983) with a recycle delay of 70 ms. Apodization of the free induction decays introduced 50 Hz line broadening. For the low-spin derivatives (metMbCN), 10 000 transients were collected over a 38.5 kHz band width with 4096 data points and a recycle delay of 120 ms. The spectra were zero filled to 8192 points and apodized to introduce 0.5−5 Hz line broadening. Chemical shifts were referenced to 2,2-dimethyl-2-silapentane-5-sulfonate (DSS) through the residual water resonance. Titrations were carried out in unbuffered 0.1 M NaCl. The pH of protein samples was measured with a Radiometer Model 84 pH-meter and an Aldrich (#Z-11,343-3) microcombination electrode. All

readings in D_2O were uncorrected for the deuterium isotope effect and are reported as pD.

Resonance Raman Spectroscopy. Resonance Raman spectra were collected using a half-meter single spectrograph equipped with a charge-coupled device detector and a holographic super notch filter (Kim et al., 1993). Myoglobin (~200 μL, $A_{407} \sim 3$, 50 mM phosphate buffer, pH 6.0, 1 mM EDTA) was irradiated in a quartz cuvette at 413 nm with a Coherent Radiation 2000 K krypton laser (70 mW). Typically, data were collected for 5 × 20 s at a spectral slit width of 14 cm^{-1}. Spectral calibration was performed in the program SpectraCalc (Galactic Industries Corp.) using the known spectrum of cyclohexanone as a standard. Peak positions are accurate to less than or equal to ± 2 cm^{-1}.

Structure Determination. Crystals of the Ser92Asp metMb variant were grown by the hanging drop vapor diffusion method (21 °C) using 5 μL droplets containing 15 mg/mL protein, 59% saturated ammonium sulfate, 20 mM Tris-HCl, and 1 mM EDTA and adjusted to pH 6.8. Reservoirs contained the same buffer except for the addition of 67% saturated ammonium sulfate. Following droplet seeding with needle crystals grown earlier (Leung et al., 1989), new crystals appeared after 3 days and grew to 0.2 × 0.3 × 0.6 mm over a period of 3 months. These crystals are of space group $P2_1$, with $a = 64.4$ Å, $b = 28.8$ Å, $c = 36.0$ Å, and $\beta = 107.0°$, and are isomorphous to those of the wild-type protein ($a = 64.3$ Å, $b = 29.0$ Å, $c = 36.0$ Å, and $\beta = 107.1°$; Evans & Brayer, 1990).

Diffraction data were collected from a single crystal with a Rigaku R-AXIS IIC area detector system. A total of 130 oscillation frames were collected with each exposed for 35 min while being oscillated through a ϕ angle of 1.8°. Intensity data were processed to structure factor amplitudes using the R-AXIS data processing package (Higashi, 1990; Sato et al., 1992). The R_{merge} for 45 864 independent intensity measurements (11 927 unique) was 5.9%.

A starting refinement model of Ser92Asp metMb was constructed from the coordinates of the wild-type protein with residue 92 initially represented as an alanine. Structural refinement used restrained parameter least squares techniques (Hendrickson, 1985) and data in the range of 6.0−1.7 Å resolution. At two points during refinement, the entire course of the polypeptide chain of this structure was inspected with sequential fragment-deleted, $F_o - F_c$, and $2F_o - F_c$ difference electron density maps that resulted in the manual adjustment of several main chain and side chain groups. These and additional electron density maps calculated during refinement consistently indicated that the side chain of Asp92 (beyond CB) was substantially disordered. The final refined position for this side chain represents the best fit that could be obtained, but it is likely to be only the most highly populated of many conformations. Also identified, by an automated search method (Tong et al., 1994), were the positions of well-defined water molecules. All water molecules identified were manually confirmed with omit difference electron density maps.

The final structure determined for Ser92Asp metMb refined to a crystallographic *R* factor of 18.8% and displays good stereochemistry with rms deviations from ideal values for bond, angle, and planar distances of 0.015, 0.031, and 0.036 Å, respectively. Overall coordinate error is estimated to be 0.12−0.16 Å by two methods (Cruickshank, 1949, 1954; Luzzati, 1952).

Table 1: Absorption Maxima (nm) for the Ferrous and Ferric Derivatives of Ser92Asp Horse Heart Myoglobin[a]

derivative	Soret	visible
metMb	408.5 (154)	504.5 (8.79)
		634 (3.37)
deoxyMb	433.5 (107)	557.5 (11.3)
MbCO	422.5 (171)	541 (13.3)
		575 (11.9)
$metMbN_3$	420.5 (104)	542 (9.6)
		574 (7.7)
metMbCN	422.5 (104)	542 (9.8)
metMbF	407.5 (135)	496 (8.1)
		608.5 (5.6)
metMbOH	411 (97)[b]	541.5 (8.5)[b]

[a] Phosphate buffer (pH 6.0, $\mu = 0.10$ M, and 25.0 °C). Molar absorption coefficients (mM^{-1} cm^{-1}) are given in parentheses. [b] pH 11.0.

RESULTS

Mass Spectrometry. Mass spectrometry of the Ser92Asp Mb variant revealed the presence of two components. The mass of the major component (17 110 ± 2) corresponds to that expected for the Ser92Asp variant with the N-terminal methionine present ($MW_{calc} = 17\,109.93$), while the mass of the minor component (16 979 ± 2) corresponds to that of the Ser92Asp variant from which the N-terminal methionine has been cleaved ($MW_{calc} = 16\,978.55$). Similar findings have been reported previously for recombinant wild-type horse heart myoglobin (Lloyd & Mauk, 1994).

Electronic Absorption Spectra. The absorption maxima and corresponding absorption coefficients for the various ferrous and ferric derivatives of the Ser92Asp variant (Table 1) are similar to those of the wild-type protein (Scheler et al., 1957; Antonini, 1965). Only small changes in absorption maxima are observed, indicating that the electronic structure and active site coordination geometry of the variant have not been seriously perturbed.

The titration behavior of Ser92Asp metMb is similar to that of the wild-type protein. As the pH is raised, formation of a hydroxide-bound derivative is observed (not shown) (Antonini & Brunori, 1971) (eq 2):

$$\mathrm{Fe(III)-H_2O} \rightleftarrows \mathrm{Fe(III)-OH^-} + \mathrm{H^+} \qquad (2)$$

For the Ser92Asp variant, a value of 8.90 ± 0.02 was obtained [25.0 °C, $\mu = 0.10$ M (NaCl)] compared to the wild-type value of 8.8 ($\mu = 0.10$ M; Tsukahara, 1986).

EPR Spectroscopy. The low-temperature (4 K) EPR spectra of wild-type and Ser92Asp myoglobin at pH 10.0 (not shown) exhibit signals that are nearly identical to each other characteristic of high-spin (H_2O-bound) ($g = 5.92$ and 1.99 for wild-type and Ser92Asp, respectively) and low-spin iron (OH^--bound) (wild-type, $g = 2.62$, 2.16, and 1.83; Ser92Asp, $g = 2.63$, 2.15, and 1.82).

Spectroelectrochemistry. A representative family of spectra obtained for the Ser92Asp variant at various applied potentials is shown in Figure 2 along with the corresponding Nernst plot (inset). The reduction potential of the variant determined from this measurement was 72 ± 2 mV *vs* SHE (25.0 °C, pH 6.0, $\mu = 0.10$ M), which compares with a value of 64 ± 0.1 mV determined for the wild-type protein (25.0 °C, pH 6.0, $\mu = 0.10$ M; Lim, 1989).

^{1}H-NMR Spectroscopy of the MetMb Derivative. The downfield region of the 200 MHz ^{1}H-NMR spectrum of (A)

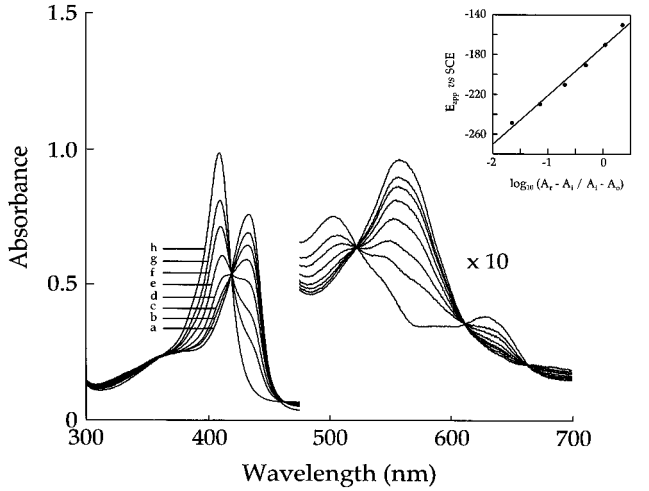

FIGURE 2: Thin-layer spectra ($[Ru(NH_3)_6Cl_3]$ = 15 μM, sodium phosphate at pH 6.0, μ = 0.10 M, 25.0 °C) of Ser92Asp myoglobin (150 μM) at various applied potentials, E_{app} (mV *vs* SCE): (a) −500.0 mV, (b) −248.8 mV, (c) −229.8 mV, (d) −210.3 mV, (e) −190.5 mV, (f) −170.0 mV, (g) −150.0 mV, and (h) +196.7 mV. The inset is a Nernst plot calculated from the spectra at 408.5 nm.

wild-type and (B) the Ser92Asp variant of horse heart metMb at pD 5.7 is shown in Figure 3. The chemical shifts of the heme methyl protons and most of the single proton resonances are similar in both proteins. As the paramagnetically induced shifts in these systems are largely contact in origin (La Mar et al., 1993), this observation implies that the unpaired spin distribution of the heme in the Ser92Asp variant is similar to that of the wild-type protein and permits tentative assignment of the hyperfine shifted resonances by comparison with the assigned resonances of wild-type sperm whale Mb (La Mar et al., 1980; Unger et al., 1985). The Ser92Asp variant exhibits a mean heme methyl shift of 76.8 ppm, compared to that of 76.5 ppm for wild-type, and a broad resonance centered at 39 ppm (peak i in Figure 3) that has been assigned previously to the heme meso protons in sperm whale Mb (La Mar et al., 1980). Both observations are consistent with a six-coordinate heme iron in Ser92Asp Mb (Rajarathnam et al., 1991) and provide evidence for the existence of a water molecule as the sixth axial ligand to the iron in this variant.

The assignments of the resonances of the pyrrole A propionate protons (peaks c, j, and l) are based on structural considerations and on their responses to changes in pH. Ser92 is in close proximity and forms a hydrogen bond to the pyrrole A propionate in the wild-type protein (Figure 1; Evans & Brayer, 1990). Replacement of this residue and the resulting elimination of this hydrogen bond might, therefore, be expected to affect the resonances of this heme substituent. The more downfield-shifted CAA proton (at 75.8 ppm; peak c) and one of the CBA protons (at 19.8 ppm; peak l) in the spectrum of the wild-type protein have moved 15.1 and 6.5 ppm upfield, respectively, in the spectrum of the Ser92Asp variant, while the other CAA propionate proton (at 31.8 ppm; peak j) shifts 14.5 ppm downfield to overlap with one of the CAD propionate protons and with the CAC vinyl proton resonances (peaks h and g). The presence of three overlapping resonances at 46.3 ppm (peaks g, h, and j) in the spectrum of the variant was confirmed by variable-temperature experiments; at 45 °C, this signal resolved as three distinct one-proton resonances (not shown). As the heme unpaired spin distribution is not substantially changed in the variant, as indicated by the nearly identical chemical

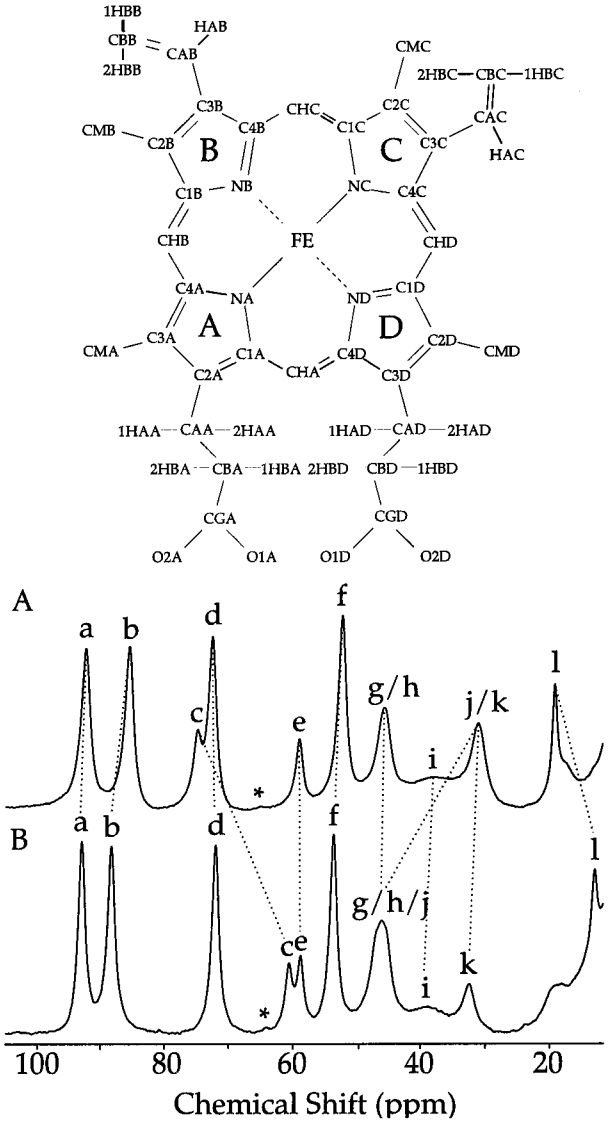

FIGURE 3: Downfield region of the 200 MHz ^{1}H-NMR spectrum of (A) wild-type and (B) Ser92Asp horse heart metMb. The assignments for the wild-type protein (La Mar et al., 1980; Unger et al., 1985) are labeled a−l (a = pyrrole A methyl protons, b = pyrrole D methyl protons, c = 1HAA or 2HAA, d = pyrrole C methyl protons, e = 1HAD or 2HAD, f = pyrrole B methyl protons, g = HAC, h = 1HAD or 2HAD, i = meso, j = 1HAA or 2HAA, k = HAB, and l = 2HBA or 1HBA), and the corresponding assignments for the variant are also indicated using the same lettering scheme. The peaks assigned to the 3-methyl resonance of the minor heme orientation in the wild-type and Ser92Asp proteins are labeled with an asterisk. Protein samples were exchanged into deuterated sodium phosphate buffer at pD 5.7 and 20 °C prior to data collection. The Brookhaven nomenclature for heme atoms used throughout this manuscript is also indicated.

shifts of the other heme resonances, such variations of specific resonances assigned to the pyrrole A propionate protons indicate that this side chain adopts a different conformation in the variant than in the wild-type protein (Rajarathnam et al., 1991; Pande et al., 1986). In contrast, the two CAD propionate protons (peaks e and h) and the HAB and HAC vinyl protons (peaks g and k) exhibit very similar shifts in the variant and in the wild-type protein, indicating that these heme substituents apparently conserve their respective conformations in the metaquo derivative of the variant.

In addition to these significant changes in chemical shift, the resonances of the pyrrole A propionate protons in Ser92Asp metMb are also sensitive to changes in pH. Many

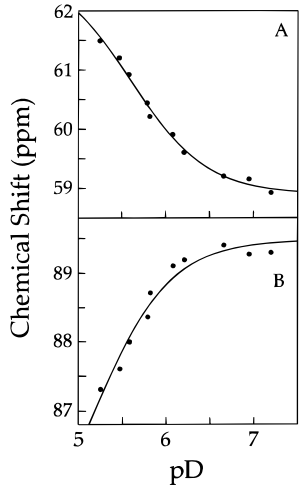

FIGURE 4: Plot of the variation of chemical shifts with pD of the (A) 1HAD or 2HAD resonance and (B) pyrrole D methyl resonances (labeled as c and b, respectively, in Figure 3) of the metMb derivative of Ser92Asp myoglobin. The solid lines represent nonlinear fits to the Henderson−Hasselbach equation (eq 1) for a single-proton process with pK_as of 5.6 ± 0.1 and 5.3 ± 0.3 for the α-proton of the pyrrole A propionate and pyrrole D methyl protons, respectively.

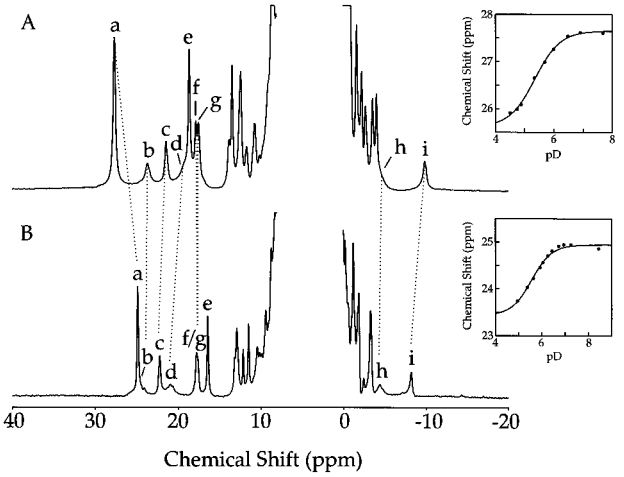

FIGURE 5: 200 MHz ^{1}H-NMR spectrum of (A) wild-type and (B) Ser92Asp horse heart metMbCN. The assignments for the wild-type protein (Emerson & La Mar, 1990a) are labeled a−i (a = pyrrole D methyl protons, b = His64 NE H, c = His93 ND1 H, d = His93 CE1 H, e = pyrrole B methyl protons, f = HAB, g = Phe43 CZ H, h = His93 CD2 H, and i = Ile99 CG H), and the corresponding assignments for the variant are indicated using the same terminology. Samples were run in sodium phosphate buffer (90% H_2O/10% D_2O) at pH 7.0 and 20 °C. The insets are plots of the variation of chemical shift of the CMD methyl resonance (indicated) with pD. The solid lines represent nonlinear fits to the Henderson−Hasselbach equation (eq 1) for a single-proton process with pK_as of 5.4 ± 0.04 and 5.6 ± 0.07 for the wild-type and Ser92Asp variant, respectively. Samples were run in 0.10 M NaCl (100% D_2O).

of the heme resonances shift slightly with changes in pD upon titration of the variant between pD 5.25 and 7.20 (not shown), but those most affected arise from the 1HAA and 2HAA hydrogens and the hydrogens of the CMD methyl group. Severe overlap of the resonance at 46.3 ppm (peak j) with two other heme resonances (Figure 3) prevents acquisition of accurate titration data for this resonance in the pD range studied. However, the change in the chemical shift of the other C2A propionate α-carbon hydrogen and the CMD methyl hydrogens (peaks c and b, respectively) with pD can be fitted to the Henderson−Hasselbach equation for a single-proton process (eq 1) to give pK_as of 5.6 ± 0.1 and 5.3 ± 0.3, respectively (Figure 4). The fact that the two calculated pK_as are within error of each other indicates that a single titrating group is responsible for the pH-dependent behavior of both of these resonances, and an averaged pK_a (calculated from the pK_as for each resonance) of 5.6 ± 0.1 is obtained. Similar titration of the wild-type protein results in chemical shifts at pH 5 and 7 that are equivalent within ±0.1 ppm (not shown).

Although an accurate estimation of the equilibrium ratio of the heme orientational isomers (La Mar et al., 1983) is difficult owing to the small amounts of the minor isomer present, examination of the ^{1}H-NMR spectra of the variant indicates that this ratio has not been substantially altered in the metMb form of the variant. The spectra of both proteins possess a signal of comparable intensity [65.1 ppm (wild-type) and 64.2 ppm (variant); labeled * in Figure 3] that has been assigned to the 3-methyl group of the minor isomer of the corresponding spectrum of sperm whale Mb (La Mar et al., 1993).

^{1}H-NMR Spectroscopy of the MetMbCN Derivative. The ^{1}H-NMR spectrum (200 MHz) of (A) wild-type and (B) Ser92Asp metMbCN in 90% H_2O/10% D_2O at pH 7.0 is shown in Figure 5. The hyperfine shifted resonances of sperm whale metMbCN have been fully assigned (Emerson & La Mar, 1990a), and those of horse heart Mb have been partially assigned by comparison (Lecomte & La Mar, 1985). The spectrum of the Ser92Asp variant exhibits features that are similar but not identical to those of horse Mb, and the tentative partial assignments of this variant are indicated (Figure 5). These assignments are based on similarities with the spectrum of the wild-type protein, on the fact that the two exchangeable resonances assigned to NE2 H of His64 and ND1 H of His93 (peaks b and c) are not observed in 100% D_2O (not shown), and on the qualitative relaxation properties of these signals as deduced from their line widths. The NE2 H of His64 [which forms a hydrogen bond to the bound cyanide (Lecomte & La Mar, 1987)] and the CE1 H and CD2 H of His93 are adjacent to the heme iron (R_{Fe-H} < 3.8 Å) and are expected to have very short relaxation times and correspondingly broad resonances.

The resonance assigned to the CG H of Ile99 (peak i), the hyperfine shift of which is purely dipolar in origin, exhibits a significantly different chemical shift (−8.0 ppm) in the variant compared to that of the wild-type protein (−9.9 ppm). This fact alone indicates that the magnetic susceptibility axes are slightly rotated from those of wild-type Mb. However, the His93 nonexchangeable protons (peaks d and h), the hyperfine shifts of which are extremely sensitive to the degree of the *z* axis tilt (Emerson & La Mar, 1990b; Rajarathnam et al., 1992, 1993, 1994), exhibit similar shifts in both proteins (Figure 5), suggesting that the relative orientation of this axis has not been perturbed significantly. As the *z* axis tilt is controlled primarily by the tilt of the bound cyanide with respect to the heme normal, which itself is imposed by steric interactions with the distal residues (Emerson & La Mar, 1990b; Rajarathnam et al., 1992, 1993, 1994), mutation of a proximal residue is not expected to affect these interactions and would, therefore, account for the similar shifts of the His93 nonexchangeable protons. On the other hand, the rhombic magnetic axes align closely with the projection of the proximal His imidazole plane onto the heme (Emerson & La Mar, 1990b). All this taken together indicates that the rhombic magnetic axes have been perturbed

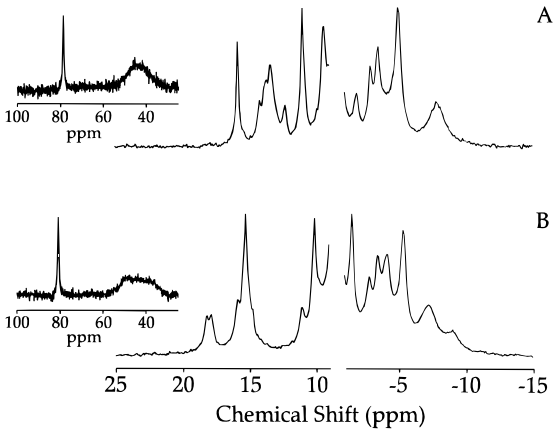

FIGURE 6: 200 MHz ^{1}H-NMR spectrum of the deoxyMb derivatives of (A) wild-type and (B) Ser92Asp horse heart myoglobins. Samples were run in sodium phosphate buffer (90% H_2O/10% D_2O) at pH 7.0 and 20 °C. The insets are the low field region showing the ND1 H (∼80 ppm), CD2 H, and CE1 H (∼44 ppm) resonances of His93.

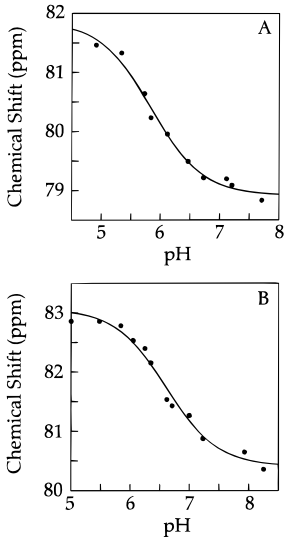

FIGURE 7: Variation of the chemical shift of the His93 ND1 resonance of (A) wild-type and (B) Ser92Asp deoxymyoglobins with pH. The solid lines represent nonlinear fits to the Henderson−Hasselbach equation (eq 1) for a single-proton process with pK_as of 5.8 ± 0.1 and 6.6 ± 0.07 for the wild-type and Ser92Asp variant, respectively.

in the metMbCN form of the variant as a consequence of a rotation of the proximal His93 ligand.

Further evidence for rotation of the proximal ligand is provided by examination of the chemical shift values. The relative orientation of His93 has a large influence on the unpaired spin density pattern on the heme, which in turn affects the contact shifts of the heme substituents. The significantly smaller chemical shifts of the pyrrole D and pyrrole B methyl protons (peaks a and e) are consistent with a rotation of His93 and, assuming a conserved porphyrin−iron bond in the variant, with a decrease of the in-plane rhombic anisotropy. In this sense, for myoglobins of various species, a clear correlation has been established between the heme methyl hyperfine shifts and the angle (θ) formed by the projection of the imidazole ring of the proximal His onto the heme plane and the line defined by the nitrogen atoms of the heme pyrroles A and C (Yamamoto et el., 1990; Soltis & Strouse, 1988). The value of θ for shark (*Galeorhinus japonicus*) Mb determined in this manner (Yamamoto et el., 1990) is intermediate between that for sperm whale Mb (θ = 19°) (Phillips, 1980) and *Aplysia limacina* Mb (θ = 29°) (Peyton et al., 1989). The chemical shifts of the assigned heme methyl resonances in Ser92Asp metMbCN are similar to those of *G. japonicus* Mb and smaller than those of wild-type horse heart protein. This finding supports the conclusion that the His93 ligand has rotated in the variant to increase θ slightly and to produce a derivative with reduced in-plane anisotropy.

The paramagnetically shifted proton resonances of the cyanide derivative of sperm whale Mb exhibit a pH dependence that can be assigned to the existence of a single titratable group with a pK_a of 5.3 (La Mar et al., 1978; Krisnamoorthi & La Mar, 1984). As for sperm whale Mb, the resonance assigned to the pyrrole D methyl group (peak a) of the wild-type and variant protein was most affected by change in pH (Figure 5, inset). The pK_a calculated from the pH dependence of the chemical shift of this resonance for the wild-type horse heart protein was 5.40 ± 0.04, and the corresponding value for the variant was 5.60 ± 0.07.

^{1}H-NMR Spectroscopy of the Deoxygenated Derivative. The ^{1}H-NMR (200 MHz) spectra of deoxygenated wild-type and Ser92Asp myoglobins in 90% H_2O/10% D_2O at pH 7.0 are shown in Figure 6. The assignments for the ^{1}H-NMR spectrum of sperm whale deoxyMb have been reported recently (La Mar et al., 1993), and the overall features for the variant are similar. In particular, the spectra of both species of protein exhibit a downfield-shifted resonance at 80.8 ppm and a broad resonance centered at 44 ppm that have been assigned to the ND1 H and the CD2 H and CE1 H atoms of the proximal His93 ligand, respectively (La Mar et al., 1993). The spectrum of the deoxyMb variant clearly demonstrates that the reduced form of the protein contains a large proportion of the so-called "minor" heme orientational isomer. The presence of signals of significant intensity in the 18 ppm region and a broad resonance at approximately −9 ppm that have been assigned to the reverse isomer in sperm whale deoxyMb (La Mar et al., 1993) are a clear indication of this fact. The identity of these resonances was confirmed by a reconstitution experiment (not shown). In a freshly reconstituted and immediately reduced (deoxygenated) sample of Ser92Asp Mb, the intensity of these signals is much greater and decreases with time until the equilibrium spectrum shown in Figure 6 is obtained. The influence of oxidation state on the heme disorder equilibrium constant will be addressed in a separate report.

The pH-dependent behavior of this variant is of interest in the context of the present work (Figure 7). For wild-type horse heart Mb, the chemical shift of the ND1 proton of His93 changes with pH in a manner consistent with a pK_a of 5.8 ± 0.1 (Figure 7A), which compares to a value of 5.6 reported for the corresponding group in wild-type sperm whale myoglobin (Krisnamoorthi & La Mar, 1984). The pK_a of this group in the Ser92Asp variant is 6.6 ± 0.1 (Figure 7B). The limiting acid and alkaline values of the His93 ND1 H chemical shifts for wild-type deoxyMb are 81.90 ± 0.02 and 78.9 ± 0.1 ppm, and the corresponding values for the variant are 83.1 ± 0.1 and 80.4 ± 0.1 ppm, respectively.

Resonance Raman Spectroscopy. The resonance Raman spectra of wild-type and Ser92Asp metMb are shown in Figure 8. Between 400 and 1700 cm^{-1}, the spectra of these two proteins are essentially indistinguishable from each other (Figure 8A). The presence of the intense ν_4 mode at 1370

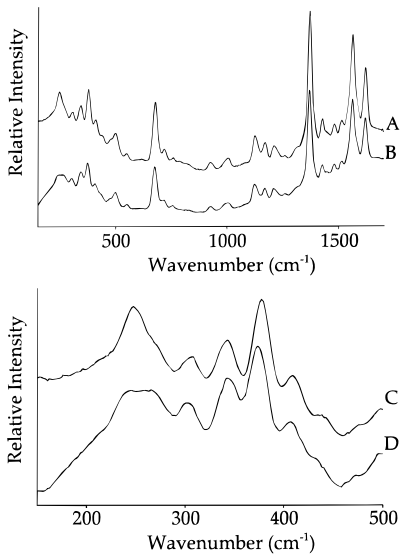

FIGURE 8: Resonance Raman spectrum of wild-type and Ser92Asp metMb (50 mM phosphate at pH 6.0). Top: 150−1700 cm^{-1} region of (A) wild-type and (B) Ser92Asp myoglobins. Bottom: expansion of the 150−500 cm^{-1} region of (C) wild-type and (D) Ser92Asp myoglobins.

cm^{-1} is characteristic of metMb in its nonphotoreduced form (Sage et al., 1989). The intense band at 1618 cm^{-1} in the spectrum of the variant indicates that there is no substantial change in vinyl group orientations relative to their positions in the wild-type protein (Sage et al., 1989). However, marked differences occur in the 200−400 cm^{-1} region (Figure 8B). The wild-type protein exhibits a principal feature at 247 cm^{-1} with a small shoulder at a higher energy, whereas the variant has at least two features (at 247 and 265 cm^{-1}) contributing to the intensity in this region. The assignment of the 247 cm^{-1} band is uncertain. Teraoka and Kitagawa (1981) attributed this feature to an Fe−imidazole stretch, but more recently, Wells et al. (1991) concluded that this band arises from a structurally sensitive out-of-plane heme mode that is intensity enhanced by heme−ligand interactions. Whatever the correct assignment, the 247 cm^{-1} band is incontrovertibly sensitive to minor conformational changes in the heme iron−histidine core.

Conformational heterogeneity of the iron−histidine bond in a number of Hb and Mb derivatives (but not metMb) has been proposed recently on the basis of band profiles of the Fe−NE2 (His93) modes and their variation with temperature (Gilch et al., 1993). These results combined with the presence of at least two features near 245 cm^{-1} in the spectrum of the Ser92Asp protein provide convincing evidence for greater conformational heterogeneity in the heme iron−histidine core than occurs in the wild-type protein. In addition, variable-temperature resonance Raman experiments (P. R. Carey and J. Doran, unpublished) with the Ser92Asp variant show marked variation in the intensity profile in the 245 cm^{-1} region between 37 and −10 °C, also consistent with the presence of multiple conformers with similar energies. Supporting evidence for the existence of conformational heterogeneity comes from close examination of the 377 cm^{-1} band (Figure 8), which has been assigned to one component of a Fermi doublet (Choi & Spiro, 1983) (the other component being the band near 345 cm^{-1}) and has been shown (Sage et al., 1989) to be sensitive to porphyrin conformational changes in metMb. The key observation in Figure 8 is that this peak shifts to a slightly lower wavenumber in the Ser92Asp variant and broadens at half-height by 11% (from 18.7 to 20.8 cm^{-1}). Peak broadening of resonance Raman profiles has been long adduced as evidence for conformational heterogeneity (Carey et al., 1973).

The resonance Raman spectra of wild-type metMb at pH 5.0 and 8.0 are indistinguishable (data not shown). The Fe−imidazole stretch region of the spectrum of the Ser92Asp variant exhibits a small variation between pH 5.0 and 8.0 (data not shown), but the two major bands at 247 and 265 cm^{-1} are present throughout this pH range and, therefore, cannot be attributed to two interconverting, pH-dependent forms of the protein.

Structure Determination. The three-dimensional atomic structures of the Ser92Asp and wild-type metMbs determined by X-ray diffraction techniques are superimposed in Figure 9A. These results, together with the matrix depicted in Figure 10, show that substitution of an aspartic acid residue at position 92 has a minimal impact on the global folding of horse heart myoglobin. The overall average positional deviation between main chain atoms in these structures is 0.21 Å, with larger shifts localized to the N- and C-termini [residue 1 (0.63 Å), residues 152 and 153 (2.3 Å)], Pro88 (0.45 Å), and Ala125 (0.42 Å). It should be noted that the N- and C-terminal residues indicated are substantially disordered, and, therefore, the differences observed are most likely a consequence of positional mobility rather than a result of the mutation. It is apparent from Figure 9 that for the most part the average main chain thermal factors of the Ser92Asp and wild-type metMbs follow similar trends. Residues 78−85 (part of the EF loop and F helix regions) are notable exceptions in that they exhibit increased mobility in the structure of the variant ($\Delta B = 5.3$ Å^2).

A detailed comparison of the Ser92Asp variant and wild-type structures in the immediate vicinity of the mutation site is illustrated in Figure 9B. As discussed earlier, the side chain of Asp92 beyond the CB atom is poorly defined in electron density maps, suggesting that it adopts a number of conformations. In the orientation found to fit the available electron density best, the χ_1 angle of Asp92 is rotated by 130° from that of the normal resident Ser92. In this conformation, Asp92 cannot form the hydrogen bonds normally formed by Ser92 with the pyrrole A propionate and ND1 of the proximal His93 heme ligand. Despite this altered hydrogen-bonding network, His93 retains almost the same positioning ($\Delta d = 0.16$ Å) in both the Ser92Asp variant and the wild-type metMb structures, along with a comparable bonding distance to the heme iron atom (2.12 Å, wild-type; 2.11 Å, Ser92Asp variant) and thermal parameters (6.9 Å^2, wild-type; 8.3 Å^2, Ser92Asp variant). One feature that may help preserve the wild-type conformation of the imidazole ring of His93 is the additional hydrogen bond from the carbonyl of Leu89 ($d = 3.0$ Å) that is preserved in the Ser92Asp variant ($d = 3.1$ Å).

The largest heme group conformational shift in the Ser92Asp variant occurs in the pyrrole A propionate, which moves away from the proximal face of the heme pocket ($\Delta d = 0.63$ Å). This change probably occurs in response to the combined loss of a former hydrogen bond to Ser92 and the proximity of the negatively charged side chain of Asp92. Along with this change is a substantial increase in the average thermal factors for the atoms of the pyrrole A propionate from an average of 10−21 Å^2 in the Ser92Asp variant. One feature that probably moderates the increase in these values

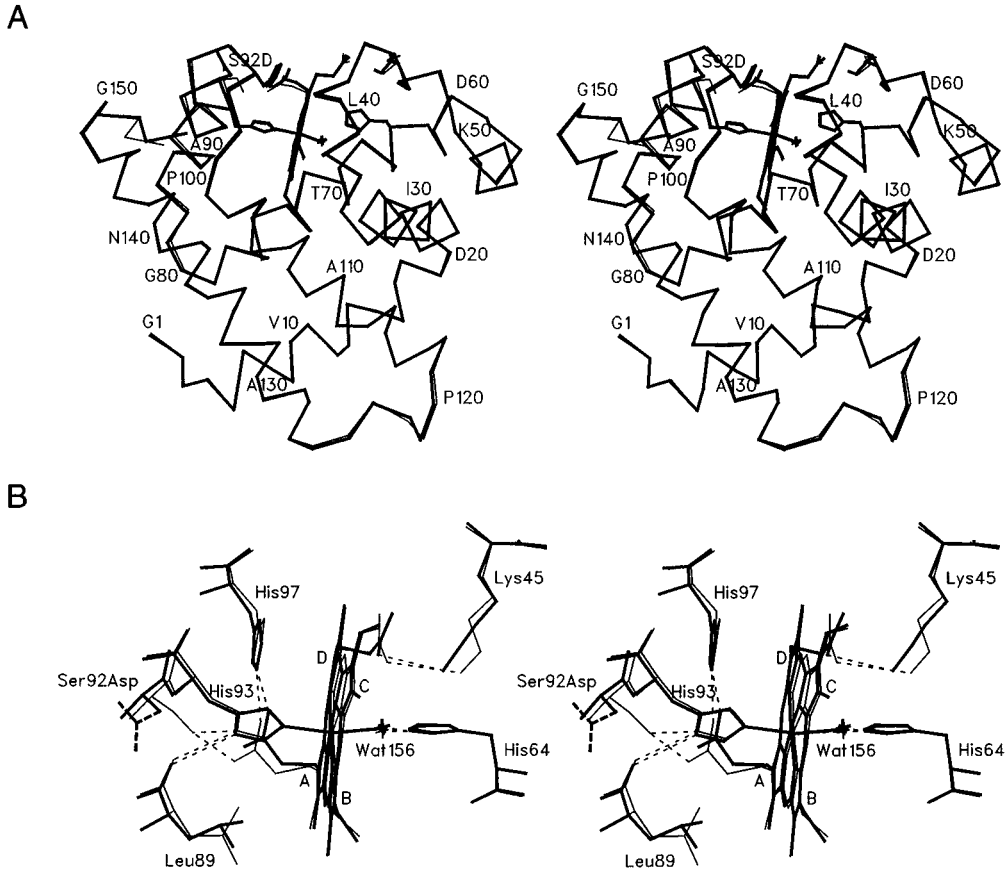

FIGURE 9: (A) Stereodrawing of the α-carbon backbones of the wild-type (thin lines) and the Ser92Asp variant (thick lines) myoglobin structures superimposed using a least squares best fit of main chain atoms. Also drawn are the side chains of the proximal ligand (His93), the distal ligand (Wat156), His64, residue 92, and both heme groups. Every tenth residue has been labeled with its one-letter amino acid designation and its sequence number. (B) Detailed stereodiagram showing the immediate environment of the Ser92Asp (thick lines) and superimposed wild-type (thin lines) structures. The disordered CB, OD1, and OD2 atoms of the Asp92 side chain and hydrogen bonds are represented with dashed lines.

in the Ser92Asp protein is the retention of the hydrogen bond from this group to His97 NE2 (2.96 Å, wild-type; 3.07 Å, Ser92Asp variant). The side chain of His97 also shows an increase in thermal parameters from an average of 8.7−14.6 Å^2 in the Ser92Asp variant. A smaller positional shift is observed in the pyrrole D heme propionate (Figure 9B) and is restricted to the rotation of its terminal carboxyl group (16°). This shift appears to coincide with a related movement of the side chain of Lys45 toward the heme plane (Δd = 0.5 Å) and leads to an increase in the average thermal factor of the atoms of the pyrrole D propionate from 16.2 to 20.9 Å^2 in the Ser92Asp structure.

DISCUSSION

Although charged amino acids have been introduced previously into the distal heme binding pocket of human Mb (Varadarajan et al., 1989a,b; Zewert et al., 1994), and the consequences of neutral amino acid substitutions (Smerdon et al., 1993; Biram et al., 1993) and axial ligand alterations on the proximal side (Adachi et al., 1991, 1993; Hildebrand et al., 1995) have been addressed, the effect of introducing electrostatically charged residues into the proximal heme binding pocket has only recently begun to attract attention. While the current work was in progress, Shiro et al. (1994) provided initial information concerning the Ser92Asp variant of a human myoglobin fusion protein, but detailed characterization was limited by poor expression and protein instability. As the Ser92Asp variant of horse heart Mb studied here exhibited no evidence of instability, we have been able to undertake a more extensive functional, structural, and spectroscopic characterization of the effects of the variant devoid of any fusion sequence.

The amino acid sequences of human and horse heart myoglobin differ at 17 positions, and of these, only residue 142 (methionine in human myoglobin and isoleucine in horse heart Mb) is located near the proximal heme binding site. We have suggested that the shorter distance between the Met142 side chain and the proximal heme ligand in the His93Tyr human variant is responsible for the observation that the side chain of Tyr93 does not flip rapidly in the human variant while it does in the corresponding horse heart variant (Hildebrand et al., 1995). It is also possible that the shorter Ile142 side chain in the horse heart protein permits greater conformational tolerance of the Asp92 residue than can be accommodated by placement of an aspartyl residue at position 92 in the human protein. This structural feature may be the basis for the greater stability of the Ser92Asp variant of the horse heart protein relative to the corresponding variant of human Mb.

Heme Electronic/Molecular Structure. The similarity of the electronic absorption spectra of various ferrous and ferric derivatives of Ser92Asp Mb with those of the wild-type protein shows that the heme electronic structure has not been altered. It has been proposed that buried point charges located in the interior of a protein molecule are able to induce large red shifts in the absorption maxima of proteins *via* electrostatic interactions between the chromophore and the ionized amino acid (Eccles & Honig, 1983). However, such

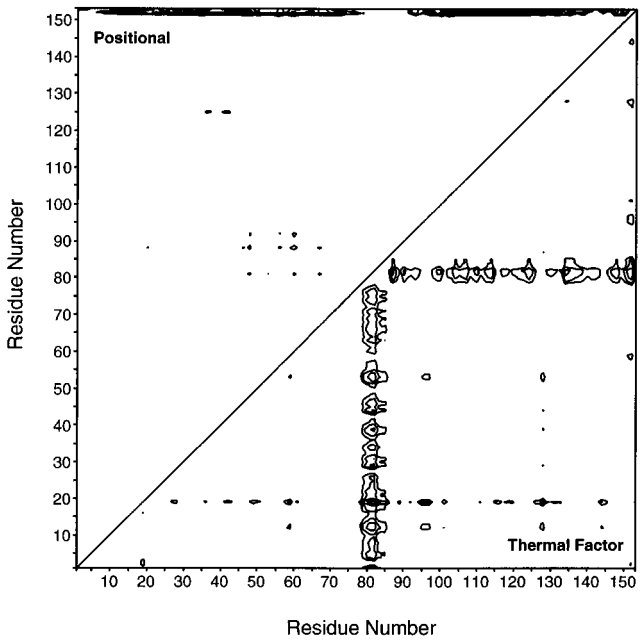

FIGURE 10: Positional and thermal factor difference matrix comparing the Ser92Asp variant and wild-type myoglobin structures. The upper left half of the matrix contains the α-carbon distance differences, and the lower right half of the same matrix contains the average main chain thermal factor differences. Since both matrices are symmetrical about the diagonal, both may be combined in this way to eliminate redundancy. The value at a given point in the thermal factor difference matrix, $P_{x,y}$, represents an amino acid pairing (x,y) and was calculated with the equation $P_{x,y} = |(B_x - B_y)_{WT} - (B_x - B_y)_{Ser92Asp}|$, where B is the average main chain thermal factor of a given amino acid residue. In the α-carbon distance difference section, the value at a point $P_{x,y}$ is calculated from $P_{x,y} = |(C_x - C_y)_{WT} - (C_x - C_y)_{Ser92Asp}|$, where C is the α-carbon coordinate of a given residue. To identify significant differences, only those 1.7 standard deviations above the mean difference are contoured for both positional and thermal factor differences. Additional 1 standard deviation intervals are also contoured. Streaks in the matrix indicate sections of polypeptide chain with significant differences in either α-carbon positioning or average main chain thermal factor. For example, residue 125 exhibits a significant α-carbon distance difference, while residues 78−85 show significant average main chain thermal factor differences. An advantage of the difference matrix method of structural comparison is that it avoids potential bias from structural superposition and differences in overall thermal factor between the structures.

effects have not been observed here or in previous studies of relevant Mb variants (Varadarajan et al., 1989a,b; Zewert et al., 1994).

The unpaired spin density pattern of the heme of Ser92Asp metaquoMb is similar to that of the wild-type protein as shown by the similarity of chemical shifts exhibited by most of the heme substituent groups (Figure 5). However, the pyrrole A propionate protons do exhibit significantly different hyperfine shifts in the variant that can be interpreted in terms of a reorientation of this side chain. This reorientation is confirmed by X-ray diffraction analysis of the structure of the Ser92Asp variant (Figure 9). The predominantly contact origin of the heme substituent hyperfine shifts in the ferric high-spin (metMb) form allows some qualitative interpretation of these shifts. The magnitude of the contact shift for an α-CH proton attached to a π system is given by eq 3 (Pande et al., 1986; La Mar, 1973):

$$(\Delta H/H)_{con} = A \cos^2 \Phi \qquad (3)$$

where A is a constant and Φ is the dihedral angle between the normal to the π system and the plane containing the carbon atom of the π system to which the substituent is attached, the α-carbon atom of the substituent and the proton. From this relationship and from the observation that the difference in the shift between the two CAA propionate protons (peaks c and j) is smaller in the Ser92Asp variant (14.4 ppm) than in the wild-type protein (43.8 ppm), with the same mean shift (53.5 and 53.1 ppm, respectively), we can conclude that the C2A−CAA bond has rotated in the variant to produce a more symmetrical disposition of the two geminal CAA protons with respect to the normal to the heme plane. According to the crystal structure of wild-type horse heart Mb (Evans & Brayer, 1990), the projection of the CAA−CBA bond is tilted toward the CMA methyl, with the CAA propionate proton closer to this methyl group experiencing the largest downfield shift (Unger et al., 1985). Therefore, the rotation of the C2A−CAA bond in the variant Mb must be in the direction of moving the CBA carbon away from the CMA methyl group.

Conformational Heterogeneity. Examination of the structure of the Ser92Asp variant (Figure 9) shows that, apart from the substituted residue, the main difference on the proximal side is a change in orientation of the pyrrole A propionate group. Although the terminal carboxylate group of the pyrrole A propionate retains a hydrogen-bonding interaction with the NE2 atom of His97, it has moved away from the proximal face of the heme, probably owing to the loss of the hydrogen bond with the OH group of Ser92 and electrostatic repulsion from the carboxylate group of the new aspartate residue at position 92. The average thermal factors of the pyrrole A propionate group have increased considerably in the variant protein (from 10.4 to 21.2 Å^2), suggesting greater conformational flexibility.

The presence of multiple conformational substates on the proximal side of the Ser92Asp variant is confirmed by resonance Raman experiments. At least two features near 247 and 265 cm^{-1} in the resonance Raman spectrum (Figure 8) demonstrate that the substitution produces a more complex conformational landscape with the coexistence of more than one heavily populated conformational state in the Asp92−heme core region. The identification of multiple conformers at pH 5.0 and 8.0 eliminates a heme-linked titratable residue (see below) as the possible cause of the heterogeneity. The time scale of the resonance Raman effect permits detection of rapidly interconverting conformers that would lead to poorly defined electron density in crystallographic experiments and a single averaged species in NMR experiments. This result also fits well with the observed positional disorder observed for the Asp92 side chain in structural studies (Figure 9B). Conformational heterogeneity has also been reported for the Ser92Leu variant of porcine Mb, for neither the carboxylate group of the pyrrole A propionate nor the CB substituents of Leu92 could be defined in electron density maps (Smerdon et al., 1993). Therefore, it appears that substitution of Ser92 by *either* charged *or* hydrophobic amino acids increases the structural mobility within this area of the proximal heme binding pocket.

Heme-Linked pH Titration. The existence of an NMR-detectable titratable residue near the heme in sperm whale metMbCN and deoxyMb derivatives has been known for some time (La Mar et al., 1978; Krishnamoorthi & La Mar, 1984; Carver & Bradbury, 1984). In the metMbCN derivative, the resonance most affected by the titration of this group is that of the pyrrole D methyl group. The close proximity

of the imidazole ring of His97 to pyrrole D of the heme and its methyl substituent led to the proposal that this residue is the heme-linked titrating group (Krishnamoorthi & La Mar, 1984; Carver & Bradbury, 1984). Nevertheless, a more recent report reinterprets these previous data and assigns this behavior to the titration of the pyrrole A propionate (La Mar et al., 1993), which forms a hydrogen bond to the NE2 of His97 (Figure 1). In view of the difficulty of differentiating between these two alternatives, the strategy of treating the propionate−His97 pair as a titrating unit as suggested by Bashford et al. (1993) is perhaps a more realistic approach at this time.

The titration of the metMbCN and deoxyMb forms of the wild-type horse heart protein exhibits behavior similar to that of the sperm whale protein and yielded pK_a values of 5.4 and 5.8, respectively. The corresponding pK_a values obtained for the cyanomet and deoxygenated forms of the variant were 5.6 and 6.6, respectively. The variant also exhibited this titration behavior in the aquomet form. Regardless of the identity of the titrating group involved, we assign this pH-dependent behavior of Ser92Asp metMb to the titration (pK_a $\sim$ 5.4) of the same residue as in the metMbCN and deoxyMb derivatives of the variant. This conclusion is consistent with the observation that, apart from the pyrrole A propionate protons, the resonance that experiences the greatest shift in both aquomet- and metMbCN derivatives of the variant is that assigned to the methyl group of pyrrole D. Because the variant protein exhibits an elevated pK_a value in the deoxygenated form relative to that exhibited by wild-type Mb, the failure of the wild-type horse heart aquomet protein to exhibit similar behavior probably results from the fact that the pK_a of this heme-linked ionizable group occurs at a pH where the wild-type protein is unstable. The increase in this pK_a value in the Ser92Asp variant may result from partial deprotonation of Asp92. A negative charge adjacent to the titrating group, either the pyrrole A propionate or His97, would decrease the acidity of both the carboxylate group and the imidazole group by electrostatic stabilization of the protonated form in either case. However, this explanation does not account for the similarity of pK_as exhibited by the wild-type and variant cyanmet derivatives. At present, we are unable to rationalize this observation satisfactorily. Nonetheless, the simplest assignment for the identity of the titrating residue at present would be His97 in all three derivatives (metMb, metMbCN, and deoxyMb).

Electrochemical, Spectroscopic, and Structural Correlations. The increase in the reduction potential of the Ser92Asp variant by 8 mV relative to that of the wild-type protein under comparable conditions (25 °C, pH 6.0) is surprising in view of the expectation that introduction of a negatively charged residue near the heme iron should decrease the reduction potential of the protein significantly. As reported by Varadarajan et al. (1989a,b), variants of human myoglobin possessing Asp or Glu residues at position 68 in the distal heme pocket exhibit reduction potentials that are nearly 200 mV lower than that of wild-type myoglobin. Clearly, simple electrostatic considerations alone are not sufficient to explain the behavior of the Ser92Asp variant. In an attempt to rationalize this observation, we have considered several factors that may contribute to this behavior and discuss their possible involvement as revealed by the available spectroscopic information.

Substitution of the seryl residue at position 92 eliminates the hydrogen bond formed by the OG oxygen of Ser92 and the ND1 nitrogen of the proximal His93 ligand. Replacement of Ser92 with Asp could potentially lead to hydrogen bond formation between the carboxyl group of the new residue and His93, but the positional disorder of Asp92 suggests that this hydrogen bond is weak, if it forms at all. Indeed, as shown in Figure 9B, the most populated conformer of Asp92 has the side chain of this residue projected away from His93 toward the surface of the protein. Hydrogen-bonding interactions of axial heme iron ligands such as this have been proposed to contribute to determination of reduction potentials of heme-containing proteins (Valentine et al., 1979), and this effect was subsequently demonstrated with model heme compounds (Doeff et al., 1983; O'Brien & Sweigart, 1985; Mincey & Traylor, 1979; Quinn et al., 1982). To investigate these effects in the variant, NMR spectroscopy of the deoxygenated derivative form was examined because the exchangeable ND1 proton of His93 resonates at a characteristically low field in this form of the protein (La Mar et al., 1993). In the variant, the ND1 proton resonance occurs with a downfield shift of $\sim$1.2−1.5 ppm relative to that of wild-type myoglobin at the acidic and basic extremes (direct comparison of the chemical shifts at neutral pH is not possible owing to the pH-dependent behavior of this resonance and the different pK_as in the two proteins; see Results). There are two possible mechanisms through which this proton could move downfield: (i) shortening of the Fe−NE2 (His93) σ bond or (ii) weakening of the hydrogen bond involving ND1 hydrogen and Ser92 (La Mar & de Ropp, 1982). From structural studies, it is clear that the Fe−His bond is unchanged in the variant, so we conclude that the downfield shift of the ND1 proton of His93 in the Ser92Asp horse heart variant originates from weakened or absent hydrogen-bonding interaction of the ND1 proton. In the absence of other factors, compromised hydrogen bonding to His93 decreases the "imidazolate" character of this residue and thereby stabilizes the reduced form of the protein.

Several other factors that may affect the reduction potential merit comment.

(i) Dielectric of the Heme Binding Pocket. The observation that the Asp92 side chain is disordered in the crystal indicates that the structural dynamics of the proximal heme pocket differ from those of the wild-type protein. This difference could decrease hydrophobicity of the heme pocket through greater time-averaged access of solvent molecules to the interior which in turn would decrease the reduction potential through stabilization of the oxidized protein (Kassner, 1972). Increased hydrophilic character of the heme pocket in the variant is consistent with the increased solvent accessibility of the heme reported for the Ser92Leu variant of porcine myoglobin (Smerdon et al., 1993).

(ii) Heme Orientation Equilibrium. Walker and colleagues (1988) have shown that the heme orientational isomers (La Mar et al., 1983, 1984) of cytochrome b_5 differ in their reduction potentials by 27 mV, with the minor isomer having the lower potential. Although the equilibrium constant (K_{eq} = [major]/[minor]) is similar for the metMb form of Ser92Asp and the wild-type protein, the minor form is more abundant in the deoxyMb form of the variant (data not shown). Because the time required for equilibration of the two isomers (data not shown) is similar to that required to complete the spectroelectrochemical experiment, the minor isomer present in the reduced protein may influence the observed midpoint potential. Nevertheless, the results previously reported for cytochrome b_5 (Walker et al., 1988)

suggest that the magnitude of this effect is unlikely to be greater than ~30 mV.

(iii) Heme Vinyl Group Orientation. Previously, we (Reid et al., 1986) and others (Lee et al., 1991) have discussed the evidence available concerning the variation in heme vinyl group electron-withdrawing power with heme vinyl group orientation and suggested that modulation of vinyl orientation could influence the midpoint potential of a heme protein by as much as ~50 mV. In the present case, NMR, resonance Raman, and crystallographic data all indicate that the vinyl group orientations are unperturbed in the Ser92Asp metMb variant. In the absence of information concerning the positions of these vinyl groups in the reduced form of the protein, the possible contribution of this factor must remain indeterminant at present.

(iv) Orientation of the Axial Ligands. NMR and resonance Raman spectroscopy both indicate that rotation of the proximal ligand has occurred, probably as the result of increased conformational mobility of the proximal heme pocket in the variant protein. Walker and Scheidt and their colleagues have proposed that heme centers with bisimidazole ligation may exhibit reduction potentials that are in part a function of the orientation of the axial ligands. Specifically, they suggest that heme iron centers in which the planes of the imidazole ligands are perpendicular to each other may possess reduction potentials that are 50 mV (Walker et al., 1986) or greater (Safo et al., 1991) than those of similar centers in which the planes of the imidazole ligands are parallel. Whether the orientation of the proximal imidazole ligand has a similar effect when the distal axial ligand is water has not been considered previously.

Finally, the effect of pH on this variant merits consideration in two regards. First, it is curious that the pK_a of the coordinated water molecule in the variant is unchanged by the disruption of the Ser92−His93 hydrogen bond. In the absence of any other changes, the weaker hydrogen bond should favor OH^- ligation and a lower pK_a (Satterlee et al., 1990; Ferrer et al., 1994). The unchanged pK_a for the distal water ligand in the variant could result from two equal and opposite effects: a decrease in pK_a caused by elimination of the Ser92−His93 hydrogen bond and an increase in the pK_a, resulting from the presence of a negative charge near the iron. The extent to which other factors, such as increased accessibility to solvent, may also contribute cannot be quantified currently.

Second, the origin of the altered behavior of the heme-linked titratable resonance mentioned above and its possible effect on the reduction potential merit comment. NMR titrations of the Ser92Asp variant established that the pK_a for this transition is raised by 0.8 pH unit in the deoxygenated protein relative to that of wild-type Mb (Ser92Asp pK_a = 6.6, wild-type pK_a = 5.8). For the wild-type metMb derivative, no pH-linked transition was observed at pD ≥5.0, and it is likely that the pK_a for the variant (pK_a ~ 5.4) in the metMb form has been elevated by a similar amount, *i.e.* ~0.8 pH unit above the wild-type value. Since the electrochemical experiments were conducted at pH 6.0 and the relative pK_as of the variant are elevated by ~0.8 pH unit, a significantly greater proportion of the His97 residue will exist as the doubly protonated imidazole in the variant in *both* the oxidized and reduced states. The electronic coupling of His97 to the heme *via* $\pi-\pi$ overlap of the orbitals of the porphyrin and the imidazole ring that renders this residue detectable as a heme-linked group argues that the electrostatic influence of the doubly protonated His97 will be transmitted to the iron by the same mechanism and thereby increase the reduction potential through electrostatic stabilization of the reduced state.

ACKNOWLEDGMENT

We thank Professor Pieter R. Cullis for access to the NMR spectrometer, Professor Ruedi Abersold for electrospray mass spectrometry analyses, Dr. Ralf Bogumil for assistance in obtaining EPR spectra, Gary Lisnecki for help with preparative fermentation, and Nham Nguyen for skilled technical assistance.

REFERENCES

Adachi, S., Nagano, S., Watanabe, Y., Ishimori, K., & Morishima, I. (1991) *Biochem. Biophys. Res. Commun. 180*, 138−144.
Adachi, S., Nagano, S., Ishimori, K., Watanabe, Y., Morishima, I., Egawa, T., Kitagawa, T., & Makino, R. (1993) *Biochemistry 32*, 241−252.
Antonini, E. (1965) *Physiol. Rev. 45*, 123.
Antonini, M., & Brunori, E. (1971) in *Hemoglobin and Myoglobin and Their Reactions with Ligands* (Neuberger, A., & Tatum, E. L., Eds.) North Holland Publishers, Amsterdam.
Bashford, D., Case, D. A., Dalvit, C., Tennant, L., & Wright, P. E. (1993) *Biochemistry 32*, 8045−8056.
Bellelli, A., Blackmore, R. S., & Gibson, Q. H. (1990) *J. Biol. Chem. 265*, 13595−13600.
Biram, D., Garratt, C. J., & Hester, R. E. (1993) *Biochim. Biophys. Acta 1163*, 67−74.
Cameron, A. D., Smerdon, S. J., Wilkinson, A. J., Habash, J., Helliwell, J. R., Li, T., & Olson, J. S. (1993) *Biochemistry 32*, 13061−13070.
Carey, P. R., Froese, A., & Schneider, H. (1973) *Biochemistry 12*, 2198−2208.
Carver, J. A., & Bradbury, J. H. (1984) *Biochemistry 23*, 4890−4905.
Carver, T. E., Rohlfs, R. J., Olson, J. S., Gibson, Q. H., Blackmore, R. S., Springer, B. A., & Sligar, S. G. (1990) *J. Biol. Chem. 265*, 20007−20020.
Choi, S., & Spiro, T. G. (1983) *J. Am. Chem. Soc. 105*, 3683−3692.
Cruickshank, D. W. J. (1949) *Acta Crystallogr. 2*, 65−82.
Cruickshank, D. W. J. (1954) *Acta Crystallogr. 7*, 519.
Cutler, R. L., Davies, A. M., Creighton, S., Warshel, A., Moore, G. R., Smith, M., & Mauk, A. G. (1989) *Biochemistry 28*, 3188−3197.
Davies, A. M., Guillemette, J. G., Smith, M., Greenwood, C., Thurgood, A. G., & Mauk, A. G. (1993) *Biochemistry 32*, 5431−5435.
de Duve, C. (1948) *Acta Chem. Scand. 2*, 264−289.
Doeff, M. M., Sweigart, D. A., & O'Brien, P. (1983) *Inorg. Chem. 22*, 851−852.
Dutton, P. L. (1978) *Methods Enzymol. 54*, 411−418.
Eccles, J., & Honig, B. (1983) *Proc. Natl. Acad. Sci. U.S.A. 80*, 4959−4962.
Egeberg, K. D., Springer, B. A., Sligar, S. G., Carver, T. E., Rohlfs, R. J., & Olson, J. S. (1990) *J. Biol. Chem. 265*, 11788−11795.
Emerson, S. D., & La Mar, G. N. (1990a) *Biochemistry 29*, 1545−1556.
Emerson, S. D., & La Mar, G. N. (1990b) *Biochemistry 29*, 1556−1566.
Evans, S. V., & Brayer, G. D. (1990) *J. Mol. Biol. 213*, 885−897.
Feng, R., & Konishi, Y. (1992) *Anal. Chem. 64*, 2090−2095.
Ferrer, J. C., Turano, P., Banci, L., Bertini, I., Morris, I. K., Smith, K. M., Smith, M., & Mauk, A. G. (1994) *Biochemistry 33*, 7819−7829.
Gilch, H., Schweitzer-Stenner, R., & Dreybolt, W. (1993) *Biophys. J. 65*, 1470−1485.
Guillemette, J. G., Matsushima-Hibiya, Y., Atkinson, T., & Smith, M. (1991) *Protein Eng. 4*, 585−592.
Heineman, W. R., Norris, B. J., & Goelz, J. F. (1975) *Anal. Chem. 47*, 79−84.

Hendrickson, W. A. (1985) *Methods Enzymol. 115*, 252−270.
Higashi, T. (1990) *J. Appl. Crystallogr. 23*, 253−257.
Hildebrand, D. P., Burk, D. L., Maurus, R., Ferrer, J. C., Brayer, G. D., & Mauk, A. G. (1995) *Biochemistry 34*, 1997−2005.
Ho, C., Ed. (1982) in *Hemoglobin and Oxygen Binding*, Elsevier, New York.
Inubishi, T., & Becker, E. D. (1983) *J. Magn. Reson. 51*, 128−133.
Kassner, R. J. (1972) *Proc. Natl. Acad. Sci. U.S.A. 69*, 2263−2267.
Kim, M., Owen, H., & Carey, P. R. (1993) *Appl. Spectrosc. 49*, 1780−1783.
Krishnamoorthi, R., & La Mar, G. N. (1984) *Eur. J. Biochem. 138*, 135−140.
La Mar, G. N. (1973) in *NMR of Paramagnetic Molecules* (La Mar, G. N., Horrocks, W. D., Jr., & Holm, R. H., Eds.) pp 1−51, Academic, New York.
La Mar, G. N., & de Ropp, J. S. (1982) *J. Am. Chem. Soc. 104*, 5203−5206.
La Mar, G. N., Budd, D. L., Sick, H., & Gersonde, K. (1978) *Biochim. Biophys. Acta 537*, 270−283.
La Mar, G. N., Budd, D. L., Smith, K. M., & Langry, K. C. (1980) *J. Am. Chem. Soc. 102*, 1822−1827.
La Mar, G. N., Davis, N. L., Parish, D. W., & Smith, K. M. (1983) *J. Mol. Biol. 168*, 887−896.
La Mar, G. N., Toi, H., & Krishnamoorthi, R. (1984) *J. Am. Chem. Soc. 106*, 6395−6401.
La Mar, G. N., Davis, N. L., Johnson, R. D., Smith, W. S., Hauksson, J. B., Budd, D. L., Dalichow, F., Langry, K. C., Morris, I. K., & Smith, K. M. (1993) *J. Am. Chem. Soc. 115*, 3869−3876.
Lecomte, J. T. J., & La Mar, G. N. (1985) *Biochemistry 24*, 7388−7395.
Lecomte, J. T. J., & La Mar, G. N. (1987) *J. Am. Chem. Soc. 109*, 7219−7220.
Lee, K.-B., Jun, E., La Mar, G. N., Rezzano, I. N., Pandey, R. K., Smith, K. M., Walker, F. A., & Buttlaire, D. H. (1991) *J. Am. Chem. Soc. 113*, 3576−3583.
Leung, C. J., Nall, B. T., & Brayer, G. D. (1989) *J. Mol. Biol. 206*, 783−785.
Lim, A. R. (1989) Ph.D. Dissertation, University of British Columbia, Vancouver, Canada.
Lloyd, E., & Mauk, A. G. (1994) *FEBS Lett. 340*, 281−286.
Luzzati, V. (1952) *Acta Crystallogr. 5*, 802−810.
Mincey, T., & Traylor, T. G. (1979) *J. Am. Chem. Soc. 101*, 765−766.
Moore, G. R., & Williams, R. J. P. (1977) *FEBS Lett. 79*, 229−232.
Moore, G. R., Harris, D. E., Leitch, F. A., & Pettigrew, G. W. (1984) *Biochim. Biophys. Acta 764*, 332−342.
Moore, G. R., Pettigrew, G. W., & Rogers, N. K. (1986) *Proc. Natl. Acad. Sci. U.S.A. 83*, 4998−4999.
Northrup, S. H., Thomasson, K. A., Miller, C. M., Barker, P. D., Eltis, L. D., Guillemette, J. G., Inglis, S. C., & Mauk, A. G. (1993) *Biochemistry 32*, 6613−6623.
O'Brien, P., & Sweigart, D. A. (1985) *Inorg. Chem. 24*, 1405−1409.
Pande, U., La Mar, G. N., Lecomte, J. T. J., Ascoli, F., Brunori, M., Smith, K. M., Pandey, R. K., Parish, D. W., & Thanabal, V. (1986) *Biochemistry 25*, 5638−5646.
Paul, K. G., Theorell, H., & Åkeson, Å. (1953) *Acta Chem. Scand. 7*, 1284−1287.
Peyton, D. H., La Mar, G. N., Pande, U., Ascoli, F., Smith, K. M., Pandey, R. K., Parish, D. W., Bolognesi, M., & Brunori, M. (1989) *Biochemistry 28*, 4880−4887.
Phillips, S. E. V. (1980) *J. Mol. Biol. 142*, 531−554.
Pladzewicz, J. R., Meyer, T. J., Broomhead, J. A., & Taube, H. (1973) *Inorg. Chem. 12*, 639.
Quinn, R., Nappa, M., & Valentine, J. S. (1982) *J. Am. Chem. Soc. 104*, 2588−2595.
Rajarathnam, K., La Mar, G. N., Chiu, M. L., Sligar, S. G., Singh, J. P., & Smith, K. (1991) *J. Am. Chem. Soc. 113*, 7886−7892.
Rajarathnam, K., La Mar, G. N., Chiu, M. L., & Sligar, S. G. (1992) *J. Am. Chem. Soc. 114*, 9048−9058.
Rajarathnam, K., Qin, J., La Mar, G. N., Chiu, M. L., & Sligar, S. G. (1993) *Biochemistry 32*, 5670−5680.
Rajarathnam, K., Qin, J., La Mar, G. N., Chiu, M. L., & Sligar, S. G. (1994) *Biochemistry 33*, 5493−5501.
Reid, L. S., Taniguchi, V. T., Gray, H. B., & Mauk, A. G. (1982) *J. Am. Chem. Soc. 104*, 7516−7519.
Reid, L. S., Lim, A. R., & Mauk, A. G. (1986) *J. Am. Chem. Soc. 108*, 8917−8201.
Rodgers, K. K., & Sligar, S. G. (1991) *J. Am. Chem. Soc. 113*, 9419−9421.
Rohlfs, R. J., Mathews, A. J., Carver, T. E., Olson, J. S., Springer, B. A., Egeberg, K. D., & Sligar, S. G. (1990) *J. Biol. Chem. 265*, 3168−3176.
Safo, M., Gupta, G. P., Walker, F. A., & Scheidt, W. R. (1991) *J. Am. Chem. Soc. 113*, 5497−5510.
Sage, J. T., Morikis, D., & Champion, P. M. (1989) *J. Chem. Phys. 90*, 3015−3032.
Saito, M.-I., Lutz, R. S., Shelley, D. A., McKelvey, E. J., Mattera, R., & Hori, H. (1991) *J. Biol. Chem. 266*, 23641−23647.
Saito, M.-I., Hori, H., Andersson, L. A., Prince, R. C., Pickering, I. J., George, G. N., Sanders, C. R., Lutz, R. S., McKelvey, E. J., & Mattera, R. (1992) *J. Biol. Chem. 267*, 22843−22852.
Saito, M.-I., Dou, Y., Yonetani, T., Olson, J. S., Li, T., Regan, R., & Gibson, Q. H. (1993) *J. Biol. Chem. 268*, 6855−6857.
Sakan, Y., Ogura, T., Kitagawa, T., Fraunfelter, F. A., Mattera, R., & Ikeda-Saito, M. (1993) *Biochemistry 32*, 5815−5824.
Sato, F., Shiro, Y., Sakaguchi, Y., Suzuki, T., Iizuka, T., & Hayasha, H. (1990) *J. Biol. Chem. 265*, 2004−2010.
Sato, M., Yamamoto, M., Imada, K., Katsube, Y., Tanaka, N., & Higashi, T. (1992) *J. Appl. Crystallogr. 25*, 348−357.
Satterlee, J. D., Erman, J. E., Mauro, J. M., & Kraut, J. (1990) *Biochemistry 29*, 8797−8808.
Scheler, W., Schoffa, G., & Jung, F. (1957) *Biochem. Z. 329*, 232.
Shiro, Y., Iizuka, T., Marubayashi, K., Ogura, T., Kitagawa, T., Balasubramanian, S., & Boxer, S. G. (1994) *Biochemistry 33*, 14986−14992.
Smerdon, S. J., Dodson, G. G., Wilkinson, A. J., Gibson, Q. H., Blackmore, R. S., Carver, T. E., & Olson, J. S. (1991) *Biochemistry 30*, 6252−6260.
Smerdon, S. J., Krzywda, S., Wilkinson, A. J., Brantley, R. E., Carver, T. E., Hargrove, M. S., & Olson, J. S. (1993) *Biochemistry 32*, 5132−5138.
Soltis, S. M., & Strouse, C. E. (1988) *J. Am. Chem. Soc. 110*, 2824−2829.
Teraoka, J., & Kitagawa, T. (1981) *J. Biol. Chem. 356*, 3969−3977.
Tong, H., Berghuis, A. M., Chen, J., Luo, Y., Guss, M., Freeman, H., & Brayer, G. D. (1994) *J. Appl. Crystallogr. 27*, 421−426.
Tsukahara, K. (1986) *Inorg. Chim. Acta 124*, 199−202.
Unger, S. W., Lecomte, J. T. J., & La Mar, G. (1985) *J. Magn. Reson. 64*, 521−526.
Valentine, J. S., Sheridan, R. P., Allen, L. C., & Kahn, P. C. (1979) *Proc. Natl. Acad. Sci. U.S.A. 76*, 1009−1013.
Varadarajan, R., Zewert, T. E., Gray, H. B., & Boxer, S. G. (1989a) *Science 243*, 69−72.
Varadarajan, R., Lambright, D. G., & Boxer, S. G. (1989b) *Biochemistry 28*, 3771−3781.
Walker, F. A., Huynh, B. H., Scheidt, W. R., & Osvath, S. R. (1986) *J. Am. Chem. Soc. 108*, 5288−5297.
Walker, F. A., Emrick, D., Rivera, J. E., Hanquet, B. J., & Buttlaire, D. H. (1988) *J. Am. Chem. Soc. 110*, 6234−6240.
Wells, A. V., Sage, J. T., Morikis, D., Champion, P. M., Chui, M. L., & Sligar, S. G. (1991) *J. Am. Chem. Soc. 113*, 9655−9660.
Wittenberg, B. A., Wittenberg, J. B., & Caldwell, P. R. B. (1975) *J. Biol. Chem. 250*, 9038−9043.
Wittenberg, J. B. (1970) *Physiol. Rev. 50*, 559−636.
Yamamoto, Y., Nanai, N., Ĉhûjô, R., & Suzuki, T. (1990) *FEBS Lett. 264*, 113−116.
Zewert, T. E., Gray, H. B., & Bertini, I. (1994) *J. Am. Chem. Soc. 116*, 1169−1173.
Zoller, M. J., & Smith, M. (1987) *Methods Enzymol. 154*, 329−350.

BI9608976